

Supplementary material

Why Nanoparticles Are Trapped at Cell Junctions When Cell Density Is High?

Tongtao Yue,^a Hongyu Zhou,^b Hainan Sun,^c Shixin Li,^a Xianren Zhang,^d Dapeng Cao,^d Xin Yi^{e*} and Bing Yan^{bc*}

^a *State Key Laboratory of Heavy Oil Processing, Center for Bioengineering and Biotechnology, College of Chemical Engineering, China University of Petroleum (East China), Qingdao 266580, P.R. China.*

^b *Key Laboratory for Water Quality and Conservation of the Pearl River Delta, Ministry of Education, Institute of Environmental Research at Greater Bay, Guangzhou University, Guangzhou 510006, P.R. China. E-mail: drbingyan@yahoo.com*

^c *School of Environmental Science and Engineering, Shandong University, Jinan 250100, P.R. China.*

^d *State Key Laboratory of Organic-Inorganic Composites, Beijing University of Chemical Technology, Beijing 100029, P.R. China.*

^e *Department of Mechanics and Engineering Science, College of Engineering, Peking University, Beijing 100871, P.R. China. E-mail: xyi@pku.edu.cn*

Note 1. Details of models and the simulation method

Coarse-grained models. The simulation system includes single and multiple spherical NPs bounded by two plasma membranes. The extracellular matrix and multiprotein complex that help stabilize junctions are currently not explicitly considered in our simulations, though their effects on NP-cell interactions cannot be ignored. Each lipid molecule contains a head group with three hydrophilic beads (H), and two tails, each containing five hydrophobic beads (T). The lipid model, which represents dimyristoylphosphatidylcholine (DMPC), was proposed by Groot and Rabone and was found to form stable bilayers and show typical phase behaviors of lipid bilayers.¹ A defined number of lipids in each bilayer were defined as receptors (R), which attract ligands (L) coating on the NP surface. Given both size and diffusivity of real receptors differ from those of lipids, a more realistic rod-like receptor model was also used to simulate the interaction of a ligand-coated NP with a single membrane, and similar results were produced. The NP of a defined diameter was constructed by arranging a number of hydrophilic beads (P) in a spherical shape with a number density of three, and was constrained to move as a rigid body during the simulations. Solvent molecules (W) and other beads are not allowed to enter the NP interior.

Simulation method. Simulations in this work are based on the dissipative particle dynamics (DPD), a mesoscopic coarse-grained simulation technique with hydrodynamic interactions. The DPD method, which was first introduced to simulate the hydrodynamic behaviors of complex fluids,² is proved to be useful in studying the mesoscale behaviors of soft matter and especially biomembrane systems.³ In DPD simulations, the elementary units are soft beads whose dynamics are governed by Newton's equation of motion. The inter-bead force is composed of conservative force (F_{ij}^C), dissipative force (F_{ij}^D), and random force (F_{ij}^R). So the total force exerted on bead i by bead j can be expressed as

$$F_i = \sum_{i \neq j} (F_{ij}^C + F_{ij}^D + F_{ij}^R),$$

The conservative force representing the excluded volume effect between beads i and j is soft repulsive and is determined by

$$F_{ij}^C = a_{ij} \frac{r_{ij}}{r_c} \max\{1 - r_{ij}/r_c, 0\},$$

where a_{ij} is the maximum repulsive force constant between beads i and j , $r_{ij} = r_j - r_i$ (r_i and r_j are their positions), $r_{ij} = |r_j - r_i|$, and r_c is the cutoff radius. The value of a_{ij} is mainly determined according to the hydrophobicity of two interacting beads. For a_{ij} between beads of the same type we set $a_{WW} = a_{HH} = a_{R_H R_H} = 25$ and $a_{TT} = a_{R_T R_T} = 15$, while for those between beads of different types, we set $a_{TW} = a_{R_T W} = 80$, $a_{HT} = a_{H R_T} = a_{R_H T} = a_{R_H R_T} = 50$, and $a_{T R_T} = 15$. Note that in DPD all interactions are soft and repulsive. If the parameter is larger than 25 (the water-water interaction parameter), the interaction can be effectively regarded as repulsive. Otherwise, the interaction is attractive if the parameter is smaller than 25. To model the favorable enthalpic interaction between ligands and receptors, we set $a_{LR_H} = 0$. All the interaction parameters are summarized in Table S1†.

Table S1. The interaction parameters between each two types of beads.

a	H _{Lipid}	T _{Lipid}	H _{Receptor}	T _{Receptor}	W	NP	Ligand
H _{Lipid}	25	50	25	50	25	25	25
T _{Lipid}	50	15	50	15	80	80	80
H _{Receptor}	25	50	25	50	25	25	0-25
T _{Receptor}	50	15	50	15	80	80	80
W	25	80	25	80	25	25	25
NP	25	80	25	80	25	25	25
Ligand	25	80	0-25	80	25	25	25

The dissipative force representing viscous drag between moving beads, has the

form,

$$F_{ij}^D = -\gamma(1 - r_{ij}/r_c)^2 (v_j - v_i)/\zeta,$$

where γ is the friction coefficient, $v_{ij} = v_j - v_i$ (v_i and v_j are their velocities). This expression is chosen to conserve the momentum of each pair of beads, and thus the total momentum of the system is conserved.

The random force representing stochastic impulse is calculated by

$$F_{ij}^R = -\eta(1 - r_{ij}/r_c)^2 \theta_{ij}/\zeta,$$

where η represents the noise amplitude, and θ_{ij} is an uncorrelated random variable with zero mean and unit variance.

In the model of lipids, we used a harmonic spring force between neighboring beads in a single molecule $F_S = K_S(r_{ij} - r_{eq})/\zeta$ to ensure the integrality of lipids, where $K_S = 128$ and $r_{eq} = 0.7$ are the spring constant and the equilibrium bond length, respectively. We also used a three-body bond angle potential $U_\varphi = K_\varphi(1 - \cos(\varphi - \varphi_0))$ to depict the rigidity of lipid tails, where $K_\varphi = 10.0$ and $\varphi_0 = \pi$ are the bond bending force constant and equilibrium bond angle, respectively.

In the simulations, all the physical quantities were scaled with the cutoff radius r_c , unit bead mass m , and unit energy $k_B T$. Dimension of the simulation box was $70r_c \times 70r_c \times 70r_c$. By comparing both membrane thickness and the lipid diffusion coefficient with experimental values, the reduced length and time units can be mapped to the real units as $r_c = 0.646$ nm and $\Delta t = 16$ ps.

In conventional DPD simulations, the conservation of lipid number in a membrane patch would lead to the increase of surface tension when the flat membrane undergoes deformation, such as budding and invagination. While in real cell membranes, the large area-to-volume ratio offers sufficient excess area to release the tension. Especially for cell junctions considered here, the tensions of separate membranes are manipulated independently, thus inducing complex behaviors of confined NPs interacting with two membranes. To solve this problem, we used the N-

varied DPD simulation method, in which the targeted tension for each membrane is controlled separately by monitoring the lipid number per area (LNPA) in the boundary membrane region, which thus acts as the lipid reservoir.⁴⁻⁶ By adding or deleting lipids, the value of LNPA can be kept within a defined range ($\rho_{LNPA}^{\min} < \rho_{LNPA} < \rho_{LNPA}^{\max}$). If the local lipid area density is less than ρ_{LNPA}^{\min} , a number of lipid molecules are inserted into the boundary region, while a number of lipids are deleted from the boundary region if the density exceeds ρ_{LNPA}^{\max} . Simultaneously, a corresponding number of water solvent beads are randomly added into or deleted from the simulation box to make the whole density of beads in the simulation box constant. The addition or deletion move for each membrane was performed every 1000 time steps to allow the tension propagating to the whole membrane.

Note 2 Free energy calculation method

The composite with a NP symmetrically confined between two membranes was chosen as the initial state for a series of constrained simulations. First, an external force was exerted on the NP center to pull it along z direction. During the simulation, a number of frames were selected that correspond to the desired NP positions along membrane normal direction. Then a constrained simulation was performed on each configuration to restrain the NP within a window corresponding to the chosen position. Finally, the thermodynamic integration method was applied to analyze the free energy change as a function of NP position along membrane normal direction $z(\gamma)$, where $\gamma = 0$ when NP locates symmetrically between two membranes.^{7, 8} As the NP moved upwards or downwards, γ increased and finally reached to 1.0 when the NP reached the defined position. The free energy change, ΔF , is expressed as:

$$\Delta F = \int_0^\gamma \frac{\partial F(\gamma)}{\partial \gamma} d\gamma,$$

For each chosen value of γ , a harmonic potential was imposed on NP center to confine its motion in the z -direction:

$$U(\gamma) = k_z [Z - z(\gamma)]^2,$$

where $k_z = 150$ and $z(\gamma)$ are the spring force constant and equilibrium position of the potential, respectively. Z is the actual position of the NP center. Under the harmonic potential, the NP was forced to oscillate around $\langle z \rangle$ in the vicinity of $z(\gamma)$, where $\langle z \rangle$ is the ensemble averaged position of the NP center. To ensure that the obtained profiles were well equilibrated, a 50000 time steps DPD simulation was performed for each chosen value of γ . Then the derivative of the free energy was determined as:

$$\frac{\partial F(\gamma)}{\partial \gamma} = \left\langle \frac{\partial U(\gamma)}{\partial \gamma} \right\rangle = 2k[\langle Z \rangle - z(\gamma)] \quad z(\gamma = 0),$$

Integrating this expression allowed the change of free energy to be determined as a function of the NP position along membrane normal direction:

$$\Delta F = \int_{d(\gamma=0)}^{d(\gamma=\varepsilon)} 2k_z [z(\gamma) - \langle Z \rangle] d\gamma .$$

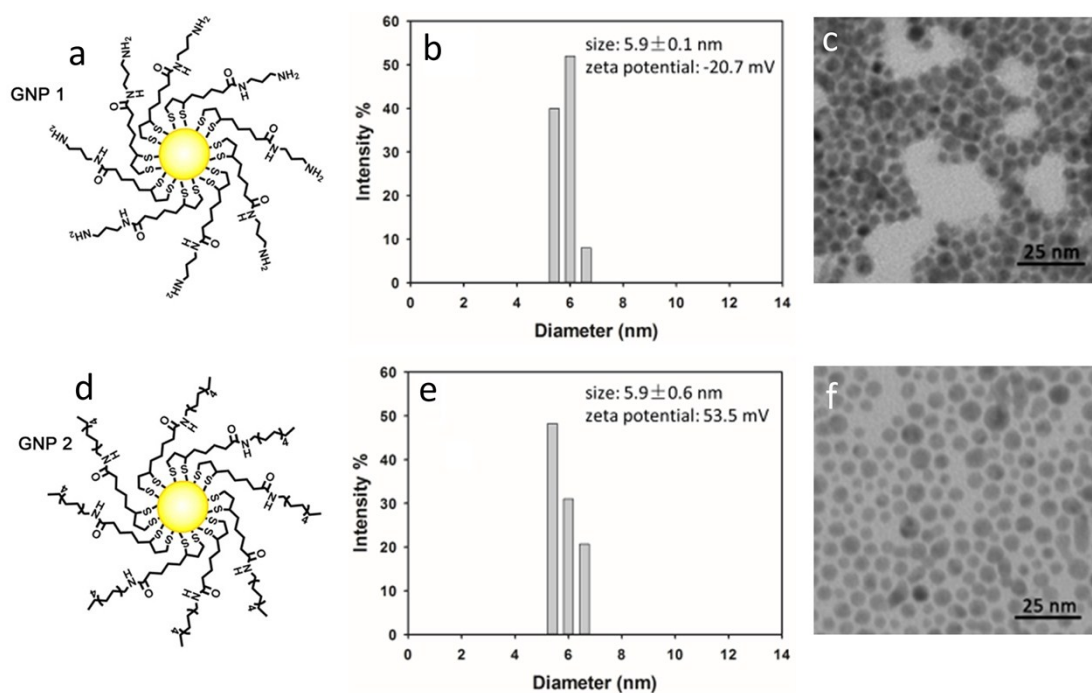


Fig. S1 Synthesis and characterization of GNPs with different hydrophobicity and surface charge. GNPs were synthesized by reduction of chloroauric acid in DMF/water in the presence of different ligands and NaBH₄. (a-c) Design of positively charge GNP (zeta-potential = 53.3 mV), size distribution (average size = 5.9 ± 0.1 nm), and representative TEM micrographs of GNPs. (d-f) Design of hydrophobic GNP, size distribution (average size = 5.9 ± 0.6 nm), and representative TEM micrographs of GNPs.

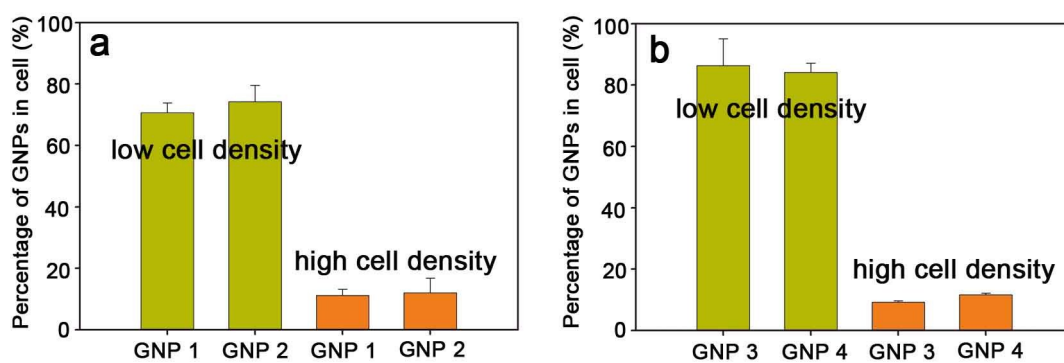


Fig. S2 Percentage of GNPs in cell at different cell densities. GNP 1 and GNP 2 ($50 \mu\text{g/mL}$) were incubated with A549 cells ($7.5 \times 10^4 \text{ cell/mL}$, $3 \times 10^5 \text{ cell/mL}$) for 24 hrs (a). GNP 3 and GNP 4 ($50 \mu\text{g/mL}$) were incubated with HeLa cells ($7.5 \times 10^4 \text{ cell/mL}$, $3 \times 10^5 \text{ cell/mL}$) for 24 hrs (b). The cellular uptake of GNPs at different cell densities was determined by ICP-MS.

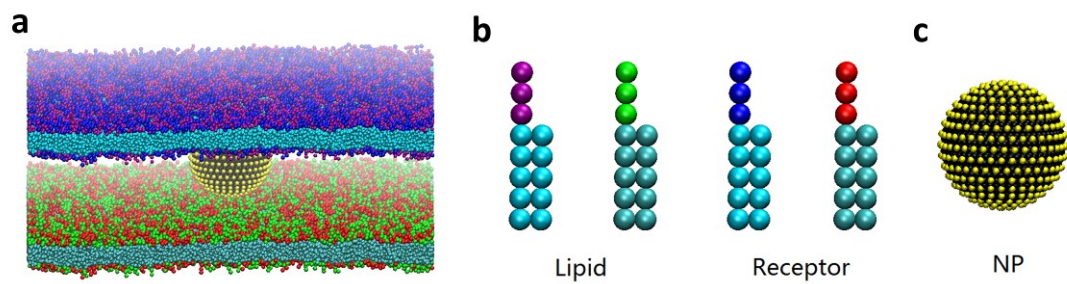


Fig. S3 Schematic representation of the interaction between NP and two parallel membranes in DPD simulations. (a) System setup includes a single spherical NP bounded by two membranes. (b) Lipid and receptor molecules in each membrane. (c) Spherical NP with a diameter of 8.6 nm coated with 425 ligands.

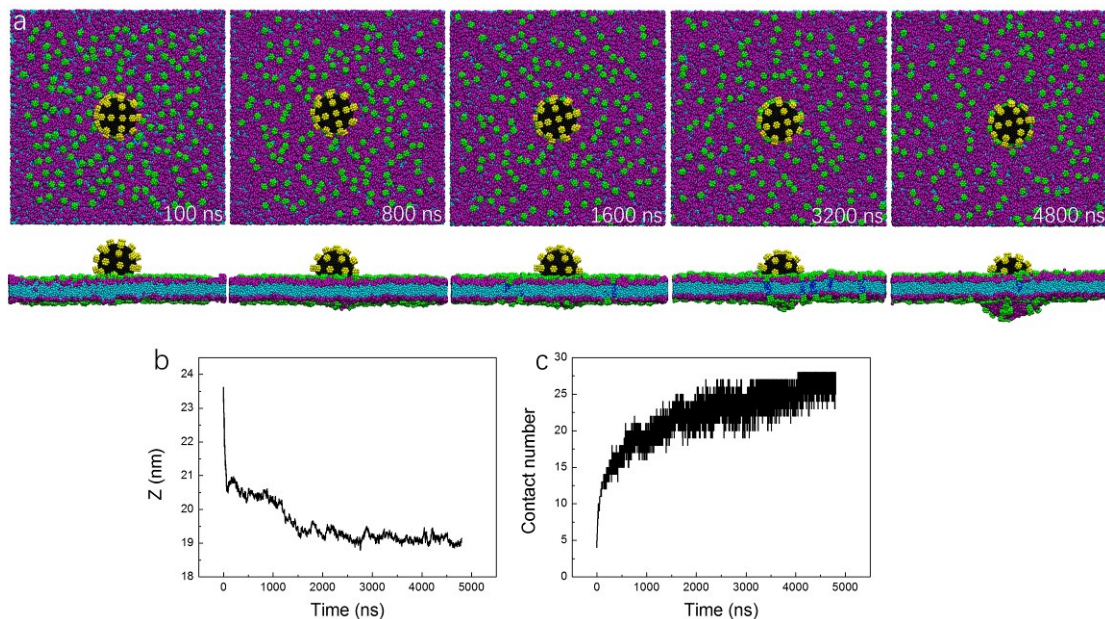


Fig. S4 Single membrane wrapping on ligand-coated NPs using a rod-like receptor model. (a-e) Time sequences of typical snapshots from both top and side views. (b) Time evolution of the NP position along z direction. (c) Time evolution of the contact number between receptors and ligands. Lipid headgroups are shown in purple, receptors are shown in green, NPs are black with the ligands shown in yellow.

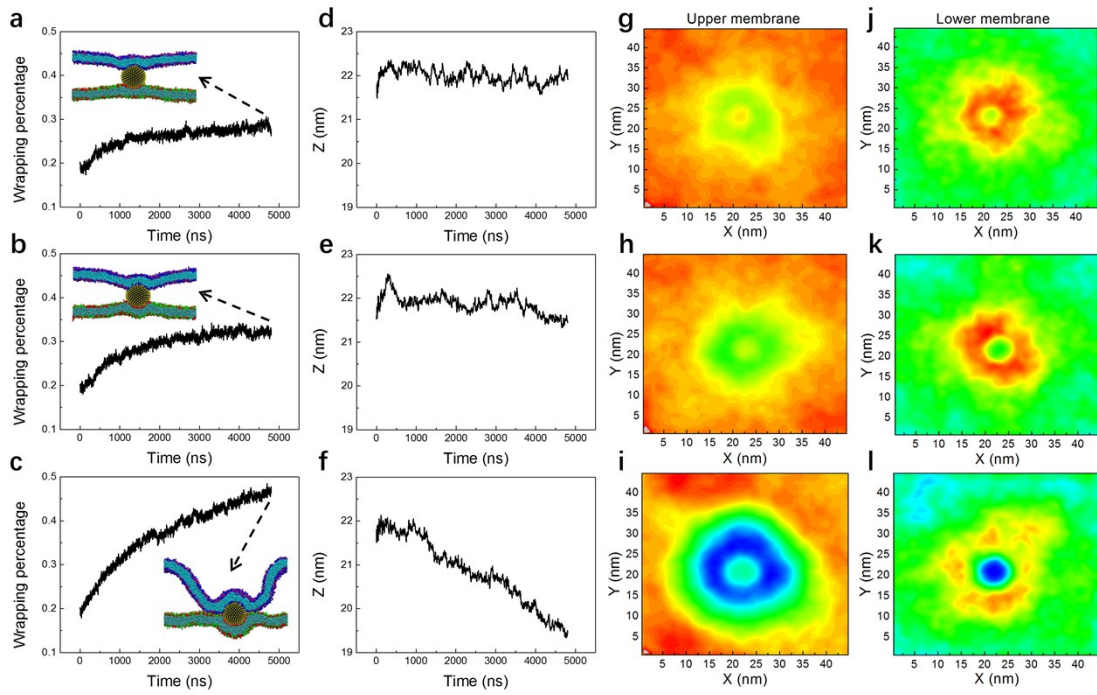


Fig. S5 Effect of membrane tension on wrapping behaviors of NPs by two symmetric membranes. (a-c) Time evolutions of the average wrapping percentage of NPs by two membranes under different tensions. Insets are the final simulated snapshots from the cross sectional view. (d-f) Time evolutions of NP positions along Z direction. (g-l) Calculated undulation of both upper and lower membranes interacting with the confined NP. The values of $\rho_{LNP A}$ for both membranes were set to be 1.5 (a, d, g, j), 1.6 (b, e, h, k), and 1.7 (c, f, i, l), respectively.

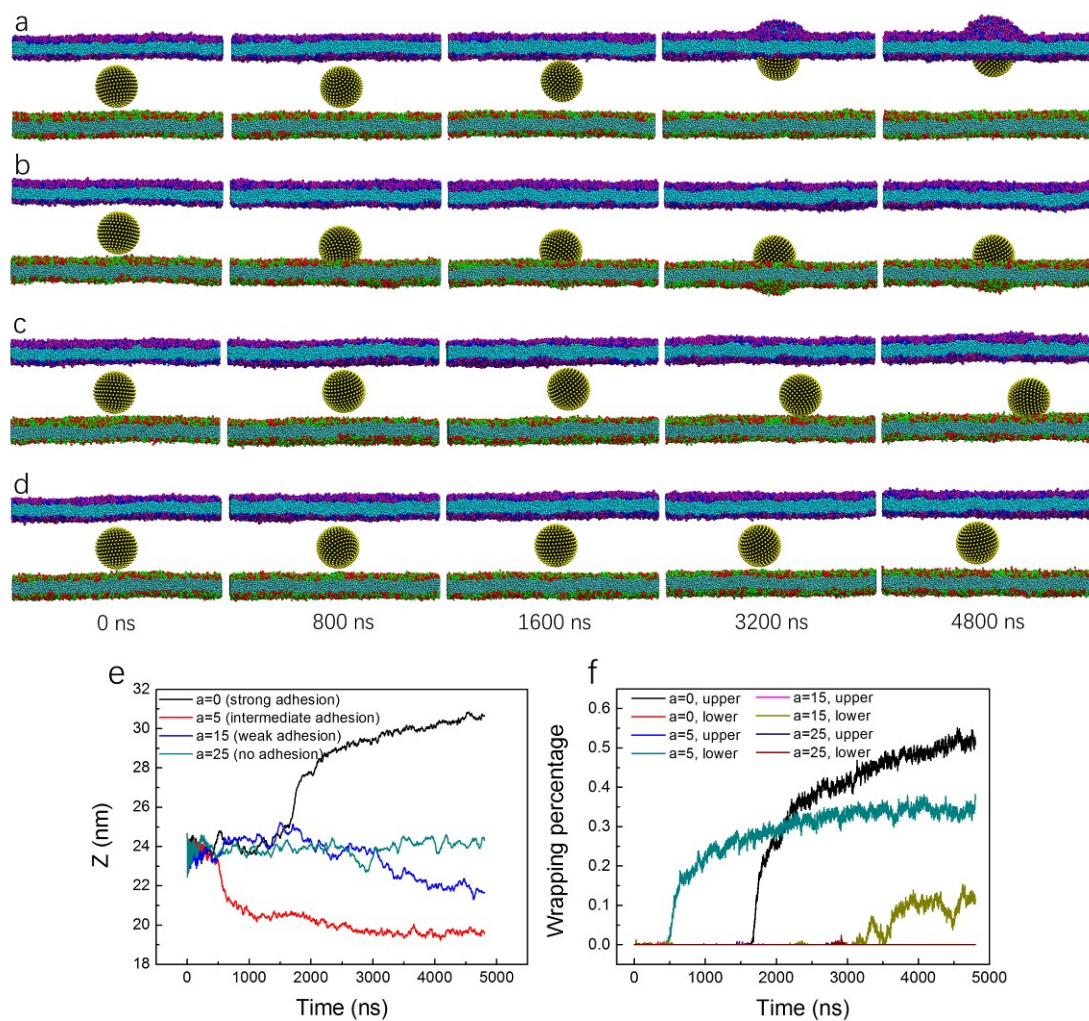


Fig. S6 Behaviors of NPs confined at a wider membrane gap under different NP-membrane adhesion strengths. (a-d) Time sequences of typical snapshots. (e) Time evolutions of NP position along z direction. (f) Time evolutions of wrapping percentages of NPs by the two membranes.

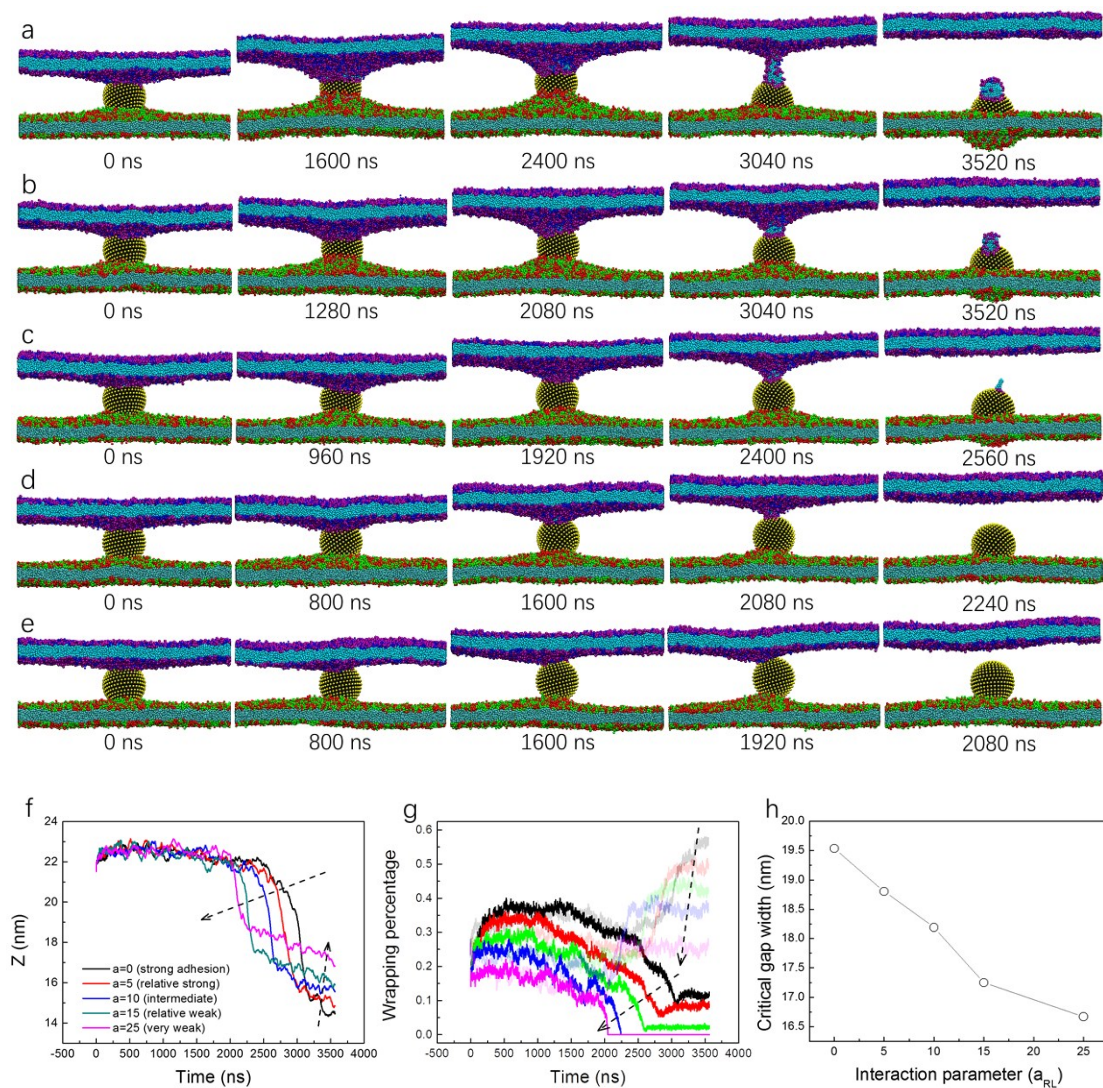


Fig. S7 Detachment of confined NPs from membrane by increasing the inter-membrane distance. (a-e) Time sequences of typical snapshots under different interaction parameters ($a_{LR_H} = 0, 5, 10, 15, 25$). (f) Time evolutions of NP positions along z direction. (g) Time evolutions of wrapping percentages of NPs by the two membranes. (h) The critical gap width for membrane detachment as a function of the interaction parameter.

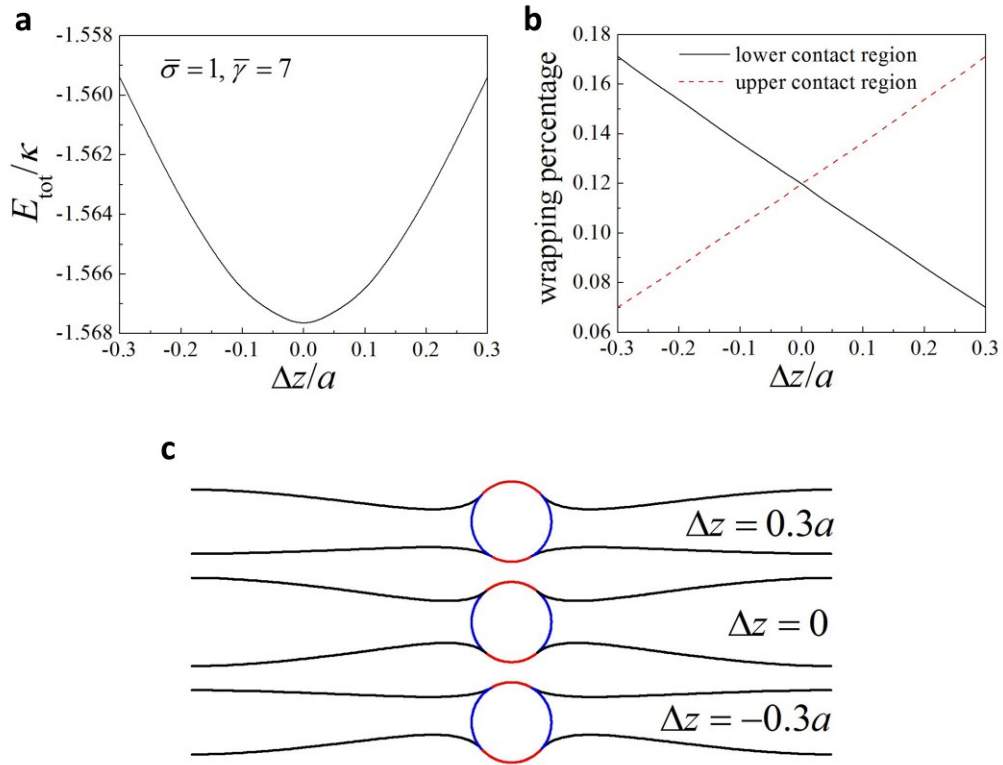


Fig. S8 Theoretical prediction of NP position confined between two membranes.

(a) E_{tot} as a function of Δz at $\bar{\sigma} = 1$ and $\bar{\gamma} = 7$ in the case of two-membrane confinement. (b) Wrapping percentage of the upper and lower contact regions as functions of Δz . (c) Selected system configurations of minimum free energy at different Δz . Taking the mirror symmetric configuration as a reference configuration, here a positive Δz means that the NP moves upwards a distance of Δz . The membrane size and distance between the remote boundaries of these two membranes are the same as those in Figure 3 in the main text.

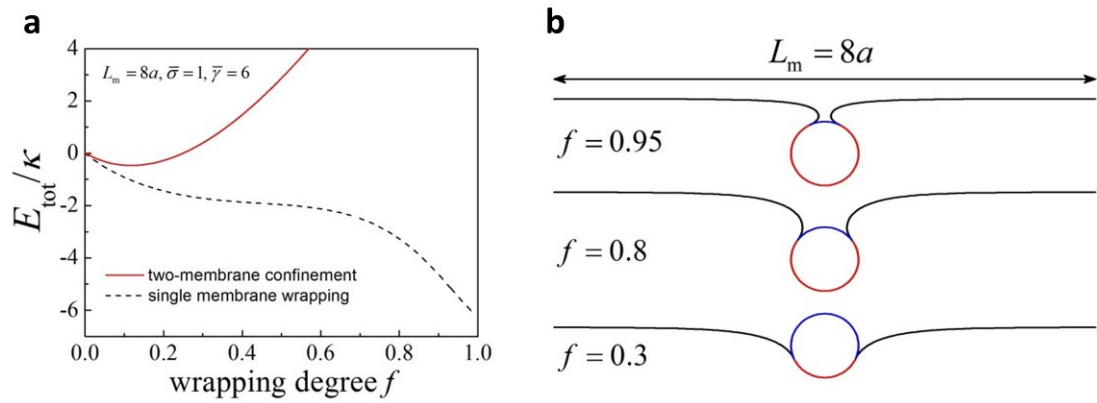


Fig. S9 Theoretical comparison of wrapping of NPs by one single membrane and two membranes. (a) Comparison of E_{tot} at $\bar{\sigma} = 1$ and $\bar{\gamma} = 6$ between the single membrane wrapping of an NP and trapping of an NP between two parallel membranes. (b) Configurations of the single membrane wrapping at different wrapping percentages f .

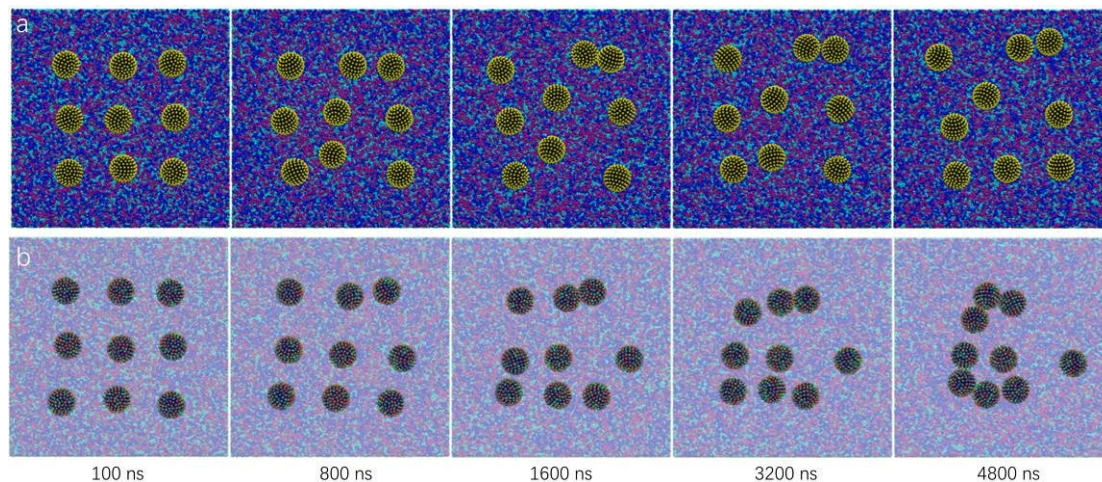


Fig. S10 Enhanced aggregation of NPs confined at cell junctions. (a) Time sequence of typical simulated snapshots showing dispersion of NPs adhering on a single membrane. (b) Time sequence of typical snapshots showing enhanced aggregation of NPs trapped at cell junctions. Surface tension of the membrane was set at $\rho_{LNP A} = 1.5$. The NP diameter is 5.2 nm.

References:

1. R. D. Groot and K. Rabone, *Biophys. J.*, 2001, **81**, 725-736.
2. R. D. Groot and P. B. Warren, *J. Chem. Phys.*, 1997, **107**, 4423.
3. J. C. Shillcock and R. Lipowsky, *Nat. Mater.*, 2005, **4**, 225-228.
4. T. Yue and X. Zhang, *ACS Nano*, 2012, **6**, 3196-3205.
5. T. Yue, X. Wang, F. Huang and X. Zhang, *Nanoscale*, 2013, **5**, 9888-9896.
6. J. Mao, P. Chen, J. Liang, R. Guo and L.-T. Yan, *ACS Nano*, 2016, **10**, 1493-1502.
7. Y. Li, X. Li, Z. Li and H. Gao, *Nanoscale*, 2012, **4**, 3768-3775.
8. T. Yue, X. Zhang and F. Huang, *Soft Matter*, 2014, **10**, 2024-2034.